Structural and Electronic Properties of the Tetraatomic B_2Be_2 Cluster

Osman F. Güner† and Koop Lammertsma*

Contribution from the Department of Chemistry, University of Alabama at Birmingham, UAB Station 219 PHS, Birmingham, Alabama 35294. *Received February 21, 1989*

Abstract: The ab initio molecular orbital study of the 10 valence electron diberyllium diboride (B_2Be_2) potential energy hypersurface yields a singlet tetrahedrallike form **1s** as the global minimum at the HF and MP2/6-31G* levels of theory. At MP4/6-31G* the energy difference of **1s** with any other isomer is at least 30 kcal/mol. The topological electron density analysis, based on the theory of atoms in molecules, shows **1s** to have its Be atoms polar π-complexed to the B–B bond with an angle of 80.1° between the π planes. The inversion barrier (**1s** ⇌ **2s** ⇌ **1s**) amounts to 11.7 kcal/mol at MP4/6-31G* + ZPE and 14.6 kcal/mol at MP2/6-311G(df) + ZPE. The D_{2h} structures **2s** and **3s** are related by means of "bond-stretch" isomerism. The electron density analysis shows that the electron density is concentrated in the center of structure **2s** whereas **3s** shows a depletion of electron density in the center as compared to the periphery of this rhombic structure. The trapezoidal **5s** and the Be-substituted B_2Be ring **4s** are discussed for their structural and electronic properties. All B_2Be_2 structures show short B–B bonds with the exception of **3s**. The effects of electron correlation and the binding energies are discussed for the global minimum.

The structures and properties of several small elemental Li,[1] Be,[2] B,[3] C,[4] Na,[5] Si,[6] S,[7] and P[8] clusters have been studied theoretically, revealing remarkable bonding patterns, as, for example, in covalent rhombic C_4 (and Si_4) and the metallic Li_n. However, the attention on binary clusters has been much more limited despite their often intriguing chemical and physical properties and their presence as binary layers in Zintl complexes. Most theoretical studies have focused on the tetraatomic A_2B_2 systems of familiar compositions. Expectantly, the A_2B_2 structures depend strongly on the number of valence electrons available. For example, the 26e (26 electrons) species O_2F_2, S_2F_2, and A_2X_2 (A = S and Se, X = Cl and Br) have nonplanar, gauche C_2 structures like hydrogen peroxide, H_2O_2, but the 18e C_2N_2 (C_2P_2) and B_2O_2 (B_2S_2) are assumed to be linear.[9] Interestingly, the linear (triplet) and rhombic isomers of the covalent tetraatomic 16e C_4 have virtually the same energy,[4] but the binary C_2Si_2 has a preference for the rhombic structure.[10] The 12e C_2Be_2 strongly favors the linear (triplet) isomer (by more than 80 kcal/mol),[11] but in the case of the ionic 10e dilithium dicarbide (C_2Li_2) the linear and rhombic structures are again of similar energy.[12] Since the type of bonding in tetraatomic clusters apparently depends on both the number of valence electrons and the electronegativity of the elements involved,[13] we were intrigued to investigate other binary systems. In this paper we discuss in detail the characteristics of the 10e B_2Be_2 cluster.

Beryllium borides are known since the turn of the century.[14] Of the many possible elemental ratios, powder patterns of three crystalline phases with compositions near BBe_2, B_2Be, and B_6Be have been reported, with a fourth phase probably resembling BBe_4.[15] Whereas compounds with a $(BBe)_n$ composition are still elusive, those with higher ratios in either boron and beryllium are known.[16] Enthalpies of formation have been reported for the crystalline clusters which are typically formed at temperatures above 1000 °C.[17] Some systems have been used in charged particle activation analysis[18a] and in the capture of negatively charged particles (pions).[18b] Beryllium borides are involved in the recently reported low-energy electronic stopping for boron in beryllium.[19] The coordination of boron and beryllium in the mineral rhodizite has been analyzed spectroscopically from the fine structure of electron-energy-loss peaks corresponding to excitations from core levels.[20] Clearly, little structural detail is available on the beryllium borides, in particular with respect to the nature of bonding.

Boron compounds are usually covalently bonded, but their structures differ from the corresponding carbon compounds.[21] For example, the borohalides B_2X_4 (X = H, F, Cl) are either ethylene-like (D_{2h}) or allene-like (D_{2d}) with strong B–B bonds that result from hyperconjugative stabilizations.[22] Due to their electron-deficient nature, boron compounds favor bridged (or

† Present address: Molecular Design Ltd., San Leandro, CA.

(1) (a) Gatti, C.; Fantucci, P.; Pacchioni, G. *Theor. Chim. Acta* **1987**, *72*, 433. (b) Rao, B. K.; Jena, P. *Phys. Rev. B* **1985**, *32*, 2058.

(2) (a) Sosa, C.; Noga, J.; Bartlett, R. J. *J. Chem. Phys.* **1988**, *88*, 5974. (b) Harrison, R. J.; Handy, N. C. *Chem. Phys. Lett.* **1986**, *123*, 321. (c) *Ibid.* **1983**, *98*, 97. (d) Lengsfield, B. H.; McLean, A. D.; Yoshimine, M.; Liu, B. *J. Chem. Phys.* **1983**, *79*, 1891. (e) Whiteside, R. A.; Raghavachari, K.; Pople, J. A.; Krogh-Jespersen, M.-B.; Schleyer, P. v. R.; Wenke, G. *J. Comput. Chem.* **1980**, *1*, 307.

(3) Whiteside, R. A. Ph.D. Dissertation, Carnegie-Mellon University, 1981; *Diss. Abstr. Int.* **1981**, *42*, 1038-B.

(4) (a) Lammertsma, K.; Güner, O. F.; Bader, R. F. W., submitted for publication. (b) Lammertsma, K.; Pople, J. A.; Schleyer, P. v. R. *J. Am. Chem. Soc.* **1986**, *108*, 7. (c) Ritchie, J. P.; King, H. F.; Young, W. S. *J. Chem. Phys.* **1986**, *85*, 5175. (d) Magers, D. H.; Harrison, R. J.; Bartlett, R. J. *J. Chem. Phys.* **1986**, *84*, 5284. (e) Rao, B. K.; Khanna, S. N.; Jena, P. *Solid State Commun.* **1986**, *58*, 53. (f) Raghavachari, K.; Whiteside, R. A.; Pople, J. A. *J. Chem. Phys.* **1986**, *85*, 6623. (g) Ewing, P. W.; Pfeiffer, G. V. *Chem. Phys. Lett.* **1982**, *86*, 365. *Ibid.* **1987**, *134*, 413. (h) Whiteside, R. A.; Krishnan, R.; DeFrees, D. J.; Pople, J. A.; Schleyer, P. v. R. *Chem. Phys. Lett.* **1981**, *78*, 538. (i) Johnston, R. L.; Hoffmann, R. *J. Am. Chem. Soc.* **1989**, *111*, 810. (j) Bernholdt, D. E.; Magers, D. H.; Bartlett, R. J. *J. Chem. Phys.* **1988**, *89*, 3612.

(5) Cao, W. L.; Gatti, C.; MacDougall, P. J.; Bader, R. F. W. *Chem. Phys. Lett.* **1987**, *141*, 380.

(6) (a) Raghavachari, K.; Rohlfing, C. M. *J. Chem. Phys.* **1988**, *89*, 2219. (b) Raghavachari, K.; Rohlfing, C. M. *Chem. Phys. Lett.* **1988**, *143*, 428. (c) Raghavachari, K. *J. Chem. Phys.* **1986**, *84*, 5672. (d) *Ibid.* **1985**, *83*, 3520. (e) Raghavachari, K.; Logovinsky, V. *Phys. Rev. Lett.* **1985**, *55*, 2853. (f) Grev, R. S.; Schaefer, H. F. *Chem. Phys. Lett.* **1985**, *119*, 111. (g) Slanina, Z. *Ibid.* **1986**, *131*, 420. (h) Balasubramanian, K. *Ibid.* **1986**, *125*, 400. (i) Diercksen, G. H. K.; Grüner, N. E.; Oddershede, J.; Sabin, J. R. *Ibid.* **1985**, *117*, 29. (j) Sabin, J. R.; Oddershede, J.; Diercksen, G. H. F.; Grüner, N. E. *J. Chem. Phys.* **1986**, *84*, 354.

(7) (a) Donahue, J. *The Structures of the Elements*; Wiley: New York, 1974; Chapter 9. (b) Steudel, R. In *Studies in Inorganic Chemistry*; Müller, A., Krebs, B., Eds.; Elsevier: Amsterdam, The Netherlands, 1984; Vol. 5, p 3. (c) Hohl, D.; Jones, R. O.; Car, R.; Parrinello, M. *J. Chem. Phys.* **1988**, *89*, 6823.

(8) (a) Ahlrichs, R.; Brode, S.; Ehrhardt, C. *J. Am. Chem. Soc.* **1985**, *107*, 7260. (b) Lazzeretti, P.; Tossell, J. A. *J. Phys. Chem.* **1987**, *91*, 800. (c) Hey, E.; Lappert, M. F.; Atwood, J. L.; Bott, S. G. *J. Chem. Soc., Chem. Commun.* **1987**, 597.

(9) Gimarc, B. M. *Molecular Structure and Bonding*; Academic Press: New York, 1979. Gimarc, B. M.; Khan, S. A.; Kohn, M. C. *J. Am. Chem. Soc.* **1978**, *100*, 1996.

(10) (a) Lammertsma, K.; Güner, O. F. *J. Am. Chem. Soc.* **1988**, *110*, 5240. (b) Trucks, G. W.; Bartlett, R. J. *THEOCHEM* **1986**, *135*, 423.

(11) Koch, W.; Frenking, G.; Gauss, J.; Cremer, D.; Sawaryn, A.; Schleyer, P. v. R. *J. Am. Chem. Soc.* **1986**, *108*, 5732.

(12) (a) Schleyer, P. v. R. *Pure Appl. Chem.* **1983**, *55*, 355. (b) Ritchie, J. P. *Tetrahedron Lett.* **1982**, *23*, 4999. (c) Ritchie, J. P.; Bachrach, S. M. *J. Am. Chem. Soc.* **1987**, *109*, 5909.

(13) Lammertsma, K. *J. Am. Chem. Soc.* **1986**, *108*, 5127.

(14) Lebeau, C. *R. Hebd. Seances Acad. Sci.* **1896**, *123*, 818.

(15) Sands, D. E.; Cline, C. F.; Zalkin, A.; Hoenig, C. L. *Acta Crystallogr.* **1961**, *14*, 309.

0002-7863/90/1512-508$02.50/0

Table I. Total (au) and Relative (kcal/mol) Energies of B_2Be_2 Isomers

			HF/3-21G//HF/3-21G				HF/6-31G*//HF/6-31G*			
structure	symmetry	state	total	rel	NIMAG	$\langle s^2 \rangle$	total	rel	NIMAG	$\langle s^2 \rangle$
1s	C_{2v}	$^1A_1$	−77.916 88	0.0	(0)		−78.373 54	0.0	(0)	
2s	D_{2h}	^1A_g	−77.898 31	11.7	(2)		−78.349 00	15.4	(2)	
2s′	C_{2h}	^1A_g	−77.900 01	10.6	(1)		−78.350 99	14.2	(1)	
3s	D_{2h}	^1A_g	−77.889 61	17.1	(0)		−78.330 38	27.1	(0)	
4s	C_s	$^1A'$	−77.886 01	19.4	(0)		−78.324 39	30.9	(1)	
5s	C_{2v}	$^1A_1$	−77.903 93	8.1	(0)		−78.344 82	18.0	(0)	
6s	C_{2v}	$^1A_1$	−77.854 42	39.2	(0)		−78.294 55	49.6	(0)	
7s	C_{2v}	$^1A_1$	−77.851 11	41.3	(2)		−78.286 69	54.5	(2)	
8s	$D_{\infty h}$	$^1\Sigma_g^+$	−77.842 06	47.0	(0)		−78.268 24	66.1	(2)	
1t	C_{2v}	$^3A_1$	−77.924 72	−4.9	(0)	2.20	−78.377 56	−2.5	(0)	2.22
2t	D_{2h}	$^3B_{3g}$	−77.911 80	3.2	(1)	2.01	−78.363 54	6.3	(1)	2.02
5t	C_{2v}	$^3A_1$	−77.908 57	5.2	(2)	2.09	−78.356 62	10.6	(2)	2.09
6t	C_{2v}	$^3A_1$	−77.837 08	50.1	(1)	2.00[a]	−78.283 15	56.7	(1)	2.00[a]
7t	C_{2v}	$^3A_1$	−77.924 84	−5.0	(0)	3.06	−78.365 90	4.8	(1)	3.20
8t	$D_{\infty h}$	$^3\Delta_g$	−77.950 00	−20.8	(0)	2.00	−78.386 83	−8.3	(0)	2.00
9t	C_s	$^3A''$	−77.927 67	−6.8	(0)	2.00[a]	−78.374 19	2.1	(1)	2.00[a]

[a] Spin-annihilated wave functions were used.

Table II. Total (au) and Relative (kcal/mol) 6-31G* Energies of B_2Be_2 Isomers[a]

		MP2		MP3		MP4		
structure	symmetry	total	rel	total	rel	total	rel	corr MP4[b]
1s	C_{2v}	−78.659 45	0.0	−78.662 46	0.0	−78.694 99	0.0	0.0
2s	D_{2h}	−78.637 00	14.1	−78.636 63	16.2	−78.675 86	12.0	10.7
2s′	C_{2h}	−78.626 12	20.9	−78.630 84	19.8	−78.664 62	19.1	18.5
3s	D_{2h}	−78.554 36	66.0	−78.577 03	53.6	−78.598 44	60.6	59.9
4s	C_s	−78.590 09	43.5	−78.595 63	41.9	−78.636 57	36.7	35.6
5s	C_{2v}	−78.564 34	59.7	−78.589 04	46.1	−78.611 25	52.5	52.0
6s	C_{2v}	−78.549 19	69.2	−78.562 55	62.7	−78.600 90	59.0	57.6
1t	C_{2v}	−78.599 20	37.8	−78.616 72	28.7	−78.638 64	35.4	34.7
2t	D_{2h}	−78.607 32	32.7	−78.619 25	27.1	−78.643 44	32.3	32.6
8t	$D_{\infty h}$	−78.573 02	71.8	−78.573 02	56.1	−78.585 23	68.9	68.1
9t	C_s	−78.592 29	42.2	−78.605 99	35.4	−78.628 13	42.0	41.3

[a] Based on HF/6-31G* optimized geometries. [b] Corrected for zero-point energies, scaled by 0.9.

nonclassical) structures.[23] This is already evident in B_2H_4 where the bis(μ-hydrido) isomer is of virtually the same energy as the anti van't Hoff isomer (D_{2d}).[24] While much less is known about beryllium compounds, they also seem to favor bridged structures[25] and even have a tendency to achieve 4-fold coordination as in $Be(BH_4)_2$.[26] A recent theoretical study on beryllium HBeX dimers showed 3-center 2-electron (3c–2e) bonds for electron-deficient, bridging X groups (i.e., BH_2, CH_3, H).[27] The Be–Be bonding appears very weak in the elemental Be clusters and in particular for the experimentally[2a-c] and theoretically[28] well-studied singlet dimer. In this paper, we rigorously address the Be–Be, B–Be, and B–B interactions in various structural isomers of the binary B_2Be_2 cluster.

Computational Methods

Ab initio molecular orbital calculations have been carried out with the GAUSSIAN series of programs.[29] The structures were completely optimized within assumed symmetries using the restricted Hartree–Fock (RHF)[30] method for singlets (indicated with s) and the unrestricted one (UHF)[31] for triplets (indicated with t).[32] Geometries were optimized using Schlegel's gradient algorithm[33] first with the split-valence 3-21G basis set[34] followed by the polarized 6-31G* basis set,[35] which has additional d-type functions for both B and Be. The effects of electron correlation were estimated by single-point calculations using the Møller–Plesset perturbation theory to the full fourth order,[36] which includes contributions of single, double, triple, and quadruple

(16) Markovsky, L. Ya.; Kondrashev, Yu. D.; Kaputovskaya, G. V. *J. Gen. Chem. USSR (Engl. Transl.)* **1955**, *25*, 1007.
(17) Morozova, M. P.; Rybakova, G. A. *Zh. Fiz. Khim.* **1974**, *48*, 1608.
(18) (a) Colin, M. E.; Friedli, C. *Radiochim. Acta* **1988**, *43*, 139. (b) Imanishi, N.; Furuya, T.; Fujiwara, I.; Shinohara, A.; Kaji, H.; Iwata, S. *Phys. Rev. A* **1985**, *32*, 2584.
(19) Gossett, C. R.; Kant, R. A.; Manning, I. *Radiat. Eff.* **1988**, *105*, 285.
(20) Brydson, R.; Vvedensky, D. D.; Engel, W.; Sauer, H.; Williams, B. G.; Zeitler, E.; Thomas, J. M. *J. Chem. Phys.* **1988**, *92*, 962.
(21) *Advances in Boron and the Boranes*; Liebman, J. F., Greenberg, A., Williams, R. E., Eds.; VCH: New York, 1988.
(22) (a) Clark, T.; Schleyer, P. v. R. *J. Comput. Chem.* **1981**, *2*, 20. (b) Vincent, M. A.; Schaefer, H. F., III *J. Am. Chem. Soc.* **1981**, *103*, 5677. (c) McKee, M. L.; Lipscomb, W. N. *J. Am. Chem. Soc.* **1981**, *103*, 4673. (d) Danielson, D. D.; Hedberg, K. *J. Am. Chem. Soc.* **1979**, *101*, 3199, and earlier references cited. (e) Zakhevskii, V. G.; Charkin, O. P. *Chem. Phys. Lett.* **1982**, *90*, 117.
(23) Lipscomb, W. N. *Boron Hydrides*; W. A. Benjamin: New York, 1983.
(24) Mohr, R. R.; Lipscomb, W. N. *Inorg. Chem.* **1986**, *25*, 1053.
(25) (a) Dill, J. D.; Schleyer, P. v. R.; Binkley, J. S.; Pople, J. A. *J. Am. Chem. Soc.* **1977**, *99*, 6159. (b) Armstrong, D. R.; Benham, H. L.; Walker, G. T. *THEOCHEM.* **1988**, *165*, 65. (c) Marynick, D. S. *J. Am. Chem. Soc.* **1981**, *103*, 1328. (d) Cimiraglia, R.; Persica, M.; Tomasi, J.; Charkin, O. P. *J. Comput. Chem.* **1984**, *5*, 263. (e) Bell, N. A.; Nowell, I. W.; Shearer, H. M. M. *J. Chem. Soc., Chem. Commun.* **1982**, 147. (f) Smith, G. S.; Johnson, Q. C.; Smith, D. K.; Cox, D. E.; Zalkin, A. *Solid State Commun.* **1988**, *67*, 491.
(26) (a) Stanton, J. F.; Lipscomb, W. N.; Bartlett, R. *J. Chem. Phys.* **1988**, *88*, 5726. (b) Charkin, O. P.; Bonaccorsi, R.; Tomasi, J.; Zyubin, A. S. *Russ. J. Inorg. Chem. (Engl. Transl.)* **1988**, *33*, 179. (c) Smith, G. S.; Johnson, Q. C.; Smith, D. K.; Cox, D. E.; Snyder, R. L.; Zhou, R.-S.; Zalkin, A. *Solid State Commun.* **1988**, *67*, 491.
(27) Hashimoto, K.; Osamura, Y.; Iwata, S. *THEOCHEM* **1987**, *152*, 101.
(28) Bondybey, V. E. *Chem. Phys. Lett.* **1984**, *109*, 436.
(29) Frisch, M. J.; Head-Gordon, M.; Schlegel, H. B.; Raghavachari, K.; Binkely, J. S.; Gonzalez, C.; Defrees, D. J.; Fox, D. J.; Whiteside, R. A.; Seeger, R.; Melius, C. F.; Baker, J.; Martin, R. L.; Kahn, L. R.; Steward, J. J. P.; Fluder, E. M.; Topiol, S.; Pople, J. A. *Gaussian 88*; Gaussian, Inc.: Pittsburgh, PA; and earlier versions.
(30) Roothan, C. C. J. *Rev. Mod. Phys.* **1951**, *23*, 69.
(31) Pople, J. A.; Nesbet, R. K. *J. Chem. Phys.* **1959**, *22*, 571.
(32) For an introduction to the methods employed, see: Hehre, W. J.; Radom, L.; Schleyer, P. v. R.; Pople, J. A. *Ab Initio Molecular Orbital Theory*; Wiley: New York, 1986.
(33) Schlegel, H. B. *J. Comput. Chem.* **1982**, *3*, 214.
(34) Binkley, J. S.; Pople, J. A.; Hehre, W. J. *J. Am. Chem. Soc.* **1980**, *102*, 939.
(35) Hehre, W. J.; Ditchfield, R.; Pople, J. A. **1972**, *56*, 2257.
(36) Krishnan, R.; Frisch, M. J.; Pople, J. A. *J. Chem. Phys.* **1980**, *72*, 4244. Møller, C.; Plesset, M. S. *Phys. Rev.* **1934**, *46*, 618.

Table III. MP2 and HF/6-31G* Vibrational Frequencies for B_2Be_2 Isomers[a]

geometries	frequencies							ZPE
1s C_{2v}	433 (a_1)	619 (a_2)	698 (b_1)	832 (b_2)	835 (a_1)	1163 (a_1)		6.5
2s D_{2h}	60*i* (b_{3u})	499 (b_{2u})	688 (a_g)	907 (b_{3g})	960 (b_{1u})	1192 (a_g)		6.1
1s C_{2v}	402 (a_1)	477 (a_2)	667 (b_1)	859 (b_2)	886 (b_2)	1136 (a_1)		6.3
2s D_{2h}	523*i* (b_{3g})	131*i* (b_{3u})	457 (b_{2u})	753 (a_g)	938 (b_{1u})	1253 (a_g)		4.9
2s' C_{2h}	100*i* (a_u)	411 (b_u)	580 (a_g)	786 (a_g)	1031 (b_u)	1116 (a_g)		5.7
3s D_{2h}	265 (b_{3u})	427 (b_{3g})	434 (a_g)	780 (b_{2u})	920 (a_g)	1061 (b_{1u})		5.6
4s C_s	65*i* (a′)	47 (a″)	558 (a′)	748 (a′)	926 (a′)	1282 (a′)		5.1
5s C_{2v}	226 (a_2)	317 (b_2)	641 (a_1)	814 (a_1)	850 (b_2)	1226 (a_1)		5.8
6s C_{2v}	94 (b_2)	113 (b_1)	299 (b_2)	644 (b_2)	937 (a_1)	1242 (a_1)		4.8
7s C_{2v}	391*i* (b_1)	147*i* (b_2)	280 (a_1)	655 (a_1)	918 (b_2)	1154 (a_1)		4.3
8s $D_{\infty h}$	119*i* (π_g)	119*i* (π_g)	34 (π_u)	34 (π_u)	685 (σ_g)	964 (σ_u)	1604 (σ_u)	4.8
1t C_{2v}	66 (b_1)	234 (a_2)	526 (a_1)	784 (a_1)	1050 (b_2)	1227 (a_1)		5.6
2t D_{2h}	109*i* (b_{3u})	703 (a_g)	956 (b_{3g})	983 (b_{2u})	1001 (a_g)	1039 (a_{2u})		6.7
5t D_{2h}	432*i* (b_2)	186*i* (a_2)	678 (a_1)	759 (b_2)	824 (a_1)	1352 (a_1)		5.2
6t C_{2v}	362*i* (b_2)	107 (b_1)	369 (a_1)	933 (a_1)	974 (b_2)	1006 (a_1)		4.8
7t C_{2v}	36*i* (b_2)	44 (b_1)	261 (a_1)	633 (a_1)	763 (b_2)	1222 (a_1)		4.2
8t $D_{\infty h}$	134 (π_u)	138 (π_u)	278 (π_g)	399 (π_g)	568 (σ_g)	821 (σ_u)	1423 (σ_u)	5.4
9t C_2	175 (a′)	242 (a″)	498 (a′)	706 (a′)	848 (a′)	1380 (a′)		5.5

[a] Only the first two entries list MP2/6-31G* frequencies.

substitutions; this level of theory is denoted as MP4(SDTQ)/6-31G*//HF/6-31G*. Single-point MCSCF calculations[37] were carried out with the GAMESS[38] program for the structures **1s** and **2s**, which were also optimized at MP2/6-31G*. These MCSCF

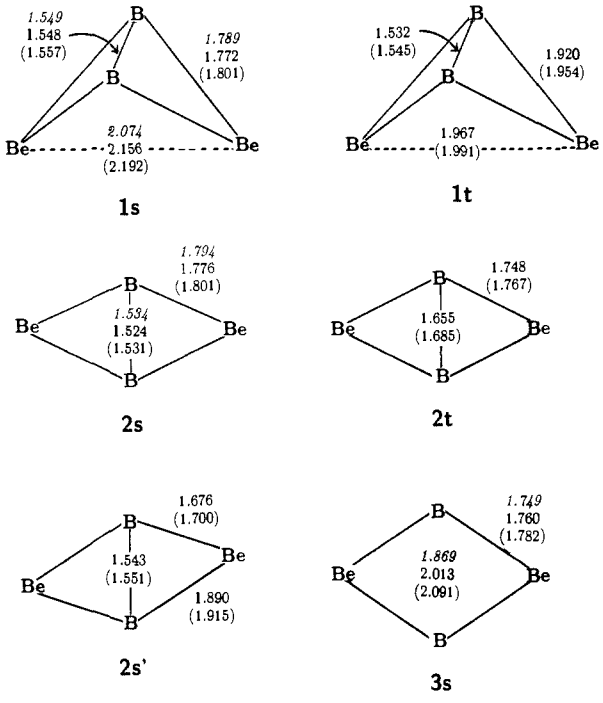

calculations were conducted by adapting an eight-orbital eight-electron valence space, which involved 1764 configurations. To evaluate the basis set dependency (for electron density analysis), additional single-point calculations were carried out at MP2/6-31+G(2d), which has two sets of 6 d-type polarization functions and an extra set of diffuse s and p functions, and with the triple split-valence 6-311G basis set augmented with a set of 6 d-type and 10 f-type functions at the MP2 level i.e., MP2/6-311G-(df)//MP2/6-31G*. For triplet structures with $\langle s^2 \rangle$ values well above 2.0, a modified GAUSSIAN version was used that annihilates this spin-contamination (AUHF).[39] Vibrational frequencies were calculated analytically at the HF/3-21G, HF/6-31G*, and MP2/6-31G* (only **1s** and **2s**) levels for characterization of stationary points as equilibria (**1s**, **1t**, **3s**, **5s**, **6s**, and **8t**), which

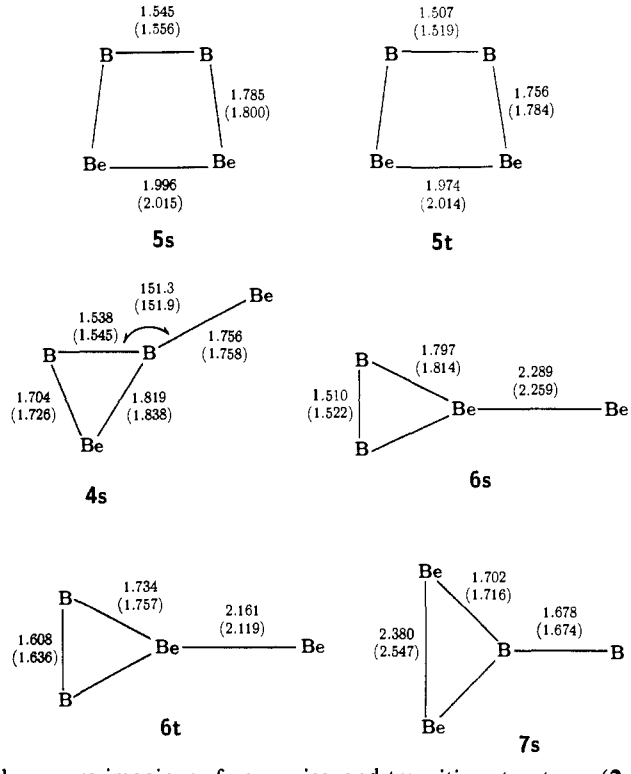

have zero imaginary frequencies, and transition structures (**2s**, **2t**, **4s**, **6t**, **7t**, and **9t**), which have one imaginary frequency; structures with two imaginary frequencies (**5t**, **7s**, and **8s**) are reported for the sake of completeness. The HF/6-31G* geometrical parameters are used throughout except for the structures **1s**, **2s**, and **3s** where MP2/6-31G* values are used unless indicated otherwise. The displayed structures show the HF/3-21G (in parentheses), the HF/6-31G*, and the MP2/6-31G* (in italics) geometries. The energies for all structures are listed in Tables I and II, with frequencies tabulated in Table III.

The bonding properties of the B_2Be_2 species have been investigated with Bader's topological electron density analysis,[40] which is based on the theory of atoms in molecules.[41] The HF and MP2/6-31G* optimized geometries and wave functions of **1s**, **2s**,

(37) Lengsfield, B. H., III *J. Chem. Phys.* **1980**, *73*, 382.
(38) GAMESS: (a) Dupuis, M.; Spangler, D.; Wendolski, J. J. *NRCC Software Catalog*; University of California: Berkeley, CA, 1980; Program QG01. (b) Schmidt, M. W.; Boatz, J. A.; Baldridge, K. K.; Koseki, S.; Gordon, M. S.; Elbert, S. T.; Lam, B. *QCPE Bull.* **1987**, *7*, 115.
(39) Kovar, T. *Diplomarbeit*; University of Erlangen-Nürnberg: Erlangen, West Germany, 1988.
(40) Bader, R. F. W. *Acc. Chem. Res.* **1985**, *18*, 9.
(41) (a) Bader, R. F. W.; Nguyen-Dang, T. T. *Adv. Quantum Chem.* **1981**, *14*, 63 and references cited therein. (b) Bader, R. F. W.; Nguyen-Dang, T. T.; Tal, Y. *Rep. Prog. Phys.* **1981**, *44*, 893 and references cited therein.

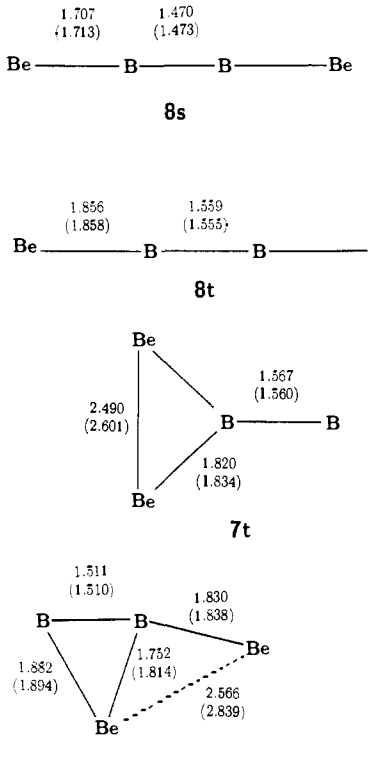

3s, **4s**, and **5s** were used to analyze the one-electron density distribution $\rho(\mathbf{r})$ with the aid of its gradient vector field $\nabla\rho(\mathbf{r})$.[42] The zero-flux lines ($\nabla\rho(\mathbf{r})\cdot n(\mathbf{r}) = 0$) define the boundaries of the basins, which are the electron density subspaces of the atoms in a molecule. In a basin the electron density $\rho(\mathbf{r})$ is always a maximum at the nuclear position. Occasionally, maxima in $\rho(\mathbf{r})$ are found at other positions, which are termed nonnuclear attractors or "pseudoatoms" since their basins do not contain nuclei.[1a,5,41b] Maxima in $\rho(\mathbf{r})$ are characterized as (3, −3) critical points ($\mathbf{r}_a$) that have three nonzero negative eigenvalues $\lambda_i(\mathbf{r})$ of the Hessian matrix $\rho(\mathbf{r})$. Critical points in $\nabla\rho(\mathbf{r})$, where $\nabla\rho(\mathbf{r}) = 0$, are classified according to rank (number of $\lambda_i \neq 0$) and signature (excess $\lambda_i > 0$ over $\lambda_i < 0$). Of particular importance are the (3, −1) or "bond-critical points" $\mathbf{r}_b$ (also termed saddle points), which have a minimum value in $\rho(\mathbf{r}_b)$ along the maximum electron density (MED) path connecting two nuclei (positive curvature); the trajectories of one of the negative curvatures define the zero-flux surfaces.[40] According to Bader,[40] "The existence of a bond path is both a necessary and sufficient condition for the existence of a bond". This definition, which does not exclude closed shell, van der Waals, and ionic interactions, was refined by Cremer and Kraka (see later) who used energy densities to define the type of bonds. Information about the σ or π character of a bond is obtained from its ellipticity ϵ at the bond critical point; the ellipticity is defined as $\epsilon = \lambda_1/\lambda_2 - 1$, where λ_1 and λ_2 are the two negative curvatures of this critical point with $\lambda_1 > \lambda_2$.[43] Bond orders $n(\mathbf{r})$ were calculated using $n(\mathbf{r}) = e^{a[\rho(\mathbf{r})-b]}$ as suggested by Cremer and Kraka.[44] By arbitrarily setting the HF/6-31G* bond order of H_2B–BH_2 (D_{2d}) equal to 1.0 and assigning a value of 2.0 to HB=BH, the constants a and b in this formula are calculated to be 4.530 and 1.187, respectively. The remaining critical points are the ring (3, +1) and cage (3, +3) critical points, which coincide with the centers of rings and cages, respectively, where the zero-flux surfaces coalesce.

The Laplacian of the charge density $\nabla^2\rho(\mathbf{r})$ of a structure determines the regions of space wherein electronic charge is locally concentrated ($\nabla^2\rho > 0$) or depleted ($\nabla^2\rho < 0$).[45] The sign of the $\nabla^2\rho(\mathbf{r})$ and the total local energy density $H(\mathbf{r})$ at a bond critical point $\mathbf{r}_b$ help in further characterizing the nature of a bond.[44,46] A bond is considered to be covalent if at the bond critical point $\nabla^2\rho$ is negative, thereby indicating concentration of charge density ρ along the bond path. Conversely, a positive value of $\nabla^2\rho$ indicates depletion of charge density in the two directions perpendicular to the bond path. Polar or ionic bonds, hydrogen bonds, and "weakly bonded" complexes, all of which involve closed-shell interactions, have positive values of $\nabla^2\rho$. However, care must be exercised in the use of $\nabla^2\rho$ as is evident in the case of F_2, which shows a positive value of $\nabla^2\rho$ at its bond critical point. Therefore, to identify bonds as ionic or covalent, Cremer and Kraka[44,46] suggested the use of local total energy densities $H(\mathbf{r})$. If $H(\mathbf{r}_b) < 0$, the charge is concentrated in the center of the bond path, thereby characterizing the bond as covalent. Conversely, when $H(\mathbf{r}_b) > 0$, the kinetic energy dominates instead of the potential energy and an ionic bond or closed-shell interaction is indicated. The existence of a *covalent bond* is then based on two conditions:[46] "(1) the existence of a (3, −1) critical point $\mathbf{r}_b$ and its associated MED path linking the nuclei in question (necessary condition) and (2) a negative value of the energy density H at the critical point $\mathbf{r}_b$ (sufficient condition)". The characteristics of the electron density analysis for **1s**, **2s**, **2s'**, **3s**, **4s**, and **5s** are listed in Tables IV and V.

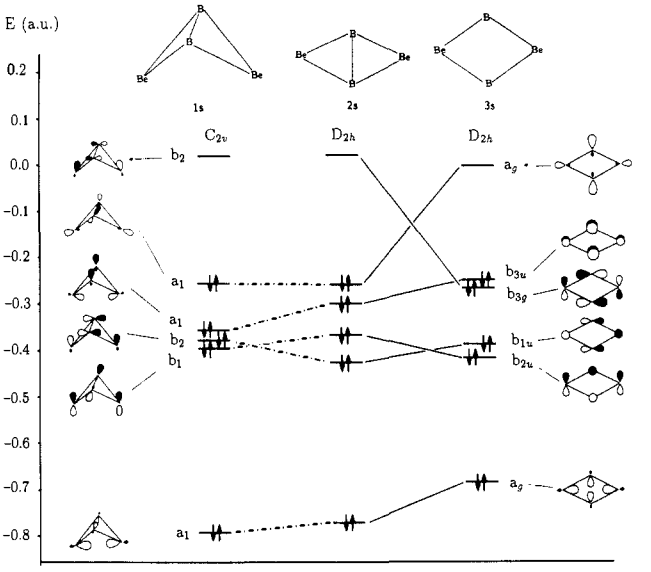

Figure 1. Valence electron HF/6-31G* MO interaction diagram for **1s**, **2s**, and **3s**.

Results and Discussion

The global minimum on the B_2Be_2 potential energy surface is a distorted tetrahedral singlet structure **1s**, which will be termed "tetrahedron" throughout the text. At first glance such a condensed structure is surprising when compared with both C_2Be_2 and the isoelectronic C_2Li_2. For instance, the lowest energy singlet C_2Be_2 isomer has a rhombic structure with a strong interaction between the inverted carbons[13] and rather polarized C–Be bonds.[11] Formal removal of two electrons from either the π or σ (mainly C–C) orbital, which is reminiscent of replacing C for B, is not expected to have a major structural influence. This argument is similar in nature to that applied for substituting C for B in [1.1.1]propellane to give the corresponding diborane compound.[47] It has been noted that the rhombic form of the 10e C_2Li_2 is highly ionic, and therefore small distortions from planarity may be easily

(42) The programs PSIG88 and EXTREME, provided by Professor R. F. W. Bader, were used to evaluate the topological properties of the electron densities. The algorithm is described in: Biegler-König, F. W.; Bader, R. F. W.; Tang, T.-H. *J. Comput. Chem.* **1982**, *3*, 317.

(43) Bader, R. F. W.; Slee, T. S.; Cremer, D.; Kraka, E. *J. Am. Chem. Soc.* **1983**, *105*, 5061.

(44) Cremer, D.; Kraka, E. *Croat. Chem. Acta* **1984**, *57*, 1259.

(45) Bader, R. F. W.; MacDougall, P. J.; Lau, C. D. H. *J. Am. Chem. Soc.* **1984**, *106*, 1594.

(46) Cremer, D.; Kraka, E. *J. Am. Chem. Soc.* **1985**, *107*, 3800.

(47) Jackson, J. E.; Allen, L. C. *J. Am. Chem. Soc.* **1984**, *106*, 591. For recent detailed studies on [1.1.1]propellane, see: Wiberg, K. B.; Bader, R. F. W.; Lau, C. D. H. *J. Am. Chem. Soc.* **1987**, *109*, 985. Feller, D.; Davidson, E. R. *Ibid.* **1987**, *109*, 4133.

Table IV. Bond Properties for B_2Be_2 Species at HF/6-31G*[a]

structure	crit pt	type	λ_1	λ_2	λ_3	ϵ	dir	$\rho(r)$	$\nabla^2\rho(r)$	$H(r)$	$n(r)$
1s	r_{a1}	(3, −3)	−4.43	−4.06	−0.97	0.09	∥	1.250	−9.47	−1.11	0.34
	r_{b2}	(3, −1)	−5.05	−4.75	8.05	0.06	∥	1.216	−1.76	−1.28	
	r_{b3}	(3, −1)	−2.20	−1.80	12.87	0.23	∥	0.569	8.87	−0.16	
2s	r_{b1}	(3, −1)	−1.23	−0.25	0.96	3.97	⊥	0.732	−0.51	−0.58	
	r_{b2}	(3, −1)	−1.24	−1.21	1.22	0.03	⊥	0.754	−1.23	−0.51	
	r_{c3}	(3, +3)	0.31	2.19	5.04	-		0.713	7.54	−0.55	
	r_{r4}	(3, +1)	−0.59	1.79	3.10	-		0.715	4.30	−0.58	
	r_{b5}	(3, −1)	−2.58	−1.42	10.51	0.82	∥	0.538	6.51	−0.19	
	r_{r6}	(3, +1)	−2.08	1.12	10.40	-		0.505	9.44	0.13	
2s′	r_{a1}	(3, −3)	−4.55	−3.54	−0.75	0.29	∥	1.194	−8.83	−1.08	1.03
	r_{b2}	(3, −1)	−4.94	−3.73	5.12	0.33	∥	1.175	−3.55	−0.12	
	r_{b3}	(3, −1)	−2.33	−1.29	0.11	0.81	∥	0.540	7.64	−0.16	
3s	r_{r1}	(3, +1)	−0.39	0.84	1.68	-		0.373	2.13	−0.11	
	r_{b2}	(3, −1)	−1.02	−0.75	2.76	0.36	⊥	0.432	0.99	−0.19	0.03
	r_{r3}	(3, +1)	−0.95	2.51	3.32	-		0.417	4.88	−0.15	
	r_{b4}	(3, −1)	−2.61	−2.56	10.85	0.02		0.551	5.69	−0.21	
4s	r_{a1}	(3, −3)	−4.77	−4.68	−0.86	0.02		1.195	−10.30	−1.08	1.04
	r_{b2}	(3, −1)	−4.74	−4.15	6.08	0.14	∥	1.171	−2.81	−1.20	
	r_{b3}	(3, −1)	−5.77	−5.52	4.97	0.04		1.178	−6.33	−1.26	
	r_{b4}	(3, −1)	−1.97	−1.35	10.25	0.46	∥	0.510	6.93	−1.55	
	r_{b5}	(3, −1)	−2.20	−2.01	8.78	0.10		0.528	4.57	−2.24	
5s	r_{a1}	(3, −3)	−7.40	−5.07	−0.22	0.46	⊥	1.260	−1.27	−1.12	1.38
	r_{b2}	(3, −1)	−8.39	−5.55	3.48	0.51	⊥	1.250	−1.05	−1.37	
	r_{b3}	(3, −1)	−2.55	−2.44	9.45	0.04		0.501	4.46	−0.19	
	r_{b4}	(3, −1)	−1.36	−1.31	2.30	0.04		0.413	−3.77	−0.22	
	r_{a5}	(3, −3)	−1.16	−1.13	0.39	0.03		0.432	−2.68	−0.22	
	r_{r6}	(3, +1)	−0.33	0.66	0.97			0.266	1.31	−0.05	

[a] λ's are in e A^{-2}; dir indicates the directions of ϵ, ∥ is parallel to the plane, ⊥ is perpendicular to the plane; $\rho(r)$ is in e A^{-3}; $\nabla^2\rho(r)$ is in e A^{-5}; $H(r)$ is in hartree A^{-3}; $n(r)$ indicates bond order.

Table V. Bond Properties for B_2Be_2 Species at Correlated MP2/6-311G(df)//MP2/6-31G* Level[a]

structure	crit pt	type	λ_1	λ_2	λ_3	ϵ	dir	$\rho(r)$	$\nabla^2\rho(r)$	$H(r)$
1s	r_{a1}	(3, −3)	−3.89	−3.71	−0.71	0.05	∥	1.207	−8.31	−1.03
	r_{b2}	(3, −1)	−4.49	−4.29	4.88,	0.04	∥	1.188	−3.90	−1.23
	r_{b3}	(3, −1)	−2.19	−1.95	11.61	0.12	∥	0.577	7.46	−0.23
2s	r_{a1}	(3, −3)	−5.16	−3.22	−0.89	0.60	∥	1.240	−9.28	−1.11
	r_{b2}	(3, −1)	−5.65	−3.90	4.73	0.45	∥	1.223	−4.83	−1.29
	r_{b3}	(3, −1)	−2.50	−1.87	10.86	0.34	∥	0.551	6.49	−0.21
3s	r_{r1}	(3, +1)	−0.31	0.99	1.33			0.452	2.00	−0.18
	r_{b2}	(3, −1)	−1.05	−1.00	2.75	0.05	⊥	0.509	0.70	−0.23
	r_{r3}	(3, +1)	−1.37	2.23	5.11			0.468	5.97	−0.19
	r_{b4}	(3, −1)	−2.77	−2.39	10.08	0.16	∥	0.571	4.93	−0.27

[a] See footnote of Table IV.

understood.[12] Consequently, the tetrahedral geometry of **1s** may imply that the interaction between its two beryllium atoms is of importance.

But let us first consider the B–B separation, which can be regarded as the backbone of **1s** just like the dicarbide unit in C_2Be_2 and C_2Li_2. The B–B distance in **1s** of 1.549 Å is shorter than that of a "typical" single bond, i.e., 1.680 Å in H_2B–BH_2 (D_{2d}),[48] but only slightly longer than the double bond of 1.510 Å in HB=BH.[48] The Mulliken overlap population[49] of 1.048, even though its use must be exercised with extreme caution,[32,50] also suggests multiple bonding between the two borons. Focusing on the berylliums, their separation of 2.075 Å can be taken as support for Be–Be bonding, since it is shorter than the 2.226-Å intermetallic bond (*a* form).[51] Also the Mulliken overlap population of 0.628 suggests (some) bonding between the two berylliums. However, this analysis must be flawed, because the other elemental separations are also short (i.e., B–Be = 1.789 Å, overlap population of 0.585), and there are simply not enough electrons available in B_2Be_2 to have bonding at all "ridges" of the tetrahedron. Of course, all bonding information must be contained in the molecular orbital framework, but analysis of bonding interactions and their ionicity is not always straightforward. The literature discussions on the transannular C–C bond in [1.1.1]propellane[4a,47] and the ionicity of C–Li bonds[12c,32,52] are exemplatory and appropriate for the case at hand. Nevertheless, the nature of the molecular orbitals (Figure 1) should be indicative of the bonding modes in **1s**. The HOMO (a_1, MO no. 9) shows strong σ interactions between the boron atomic p orbitals. The next occupied orbitals show B–B π-bonding (a_1, MO no. 8) with some attractive interaction between the beryllium nuclei and π-overlap of all berylliums and borons (b_2, MO no. 7). Clearly, the above does not lead to a detailed understanding of the tetrahedral B_2Be_2 structure. Therefore, we resort to the quantum theory of atoms in molecules through a topological analysis of the charge density function[40] at the MP2/6-31G* level.

When the charge density gradient field $\nabla\rho$ of **1s** is displayed for the plane containing both berylliums and bisecting the B–B bond (Figure 2b), no maximum electron density (MED) path is found between these Be atoms. Figure 2 shows that there exists neither a Be–Be bond nor Be–B bond paths. In fact, through the bond paths, the berylliums are connected to the midpoint of the B–B bond path. It thus appears that both berylliums are "π-bonded" to a multiple B–B bond. This is supported by the large ellipticity (0.188) of its bond critical points r_{b3} (3, −1) and their

(48) Whiteside, R. A.; Frisch, M. J.; Binkely, J. S.; DeFrees, D. J.; Schlegel, H. B.; Krishnan, R.; Pople, J. A. *Carnegie-Mellon Quantum Chemistry Archive*, 2nd ed.; Carnegie Mellon University: Pittsburgh, PA, 1981.

(49) Mulliken, R. S. *J. Chem. Phys.* **1955**, *23*, 1833, 1841, 2338, 2343.

(50) (a) Wiberg, K. B.; Wendolski, J. J. *J. Phys. Chem.* **1984**, *88*, 586. (b) Grier, D. L.; Streitwieser, A. *J. Am. Chem. Soc.* **1982**, *104*, 3556.

(51) *Handbook of Chemistry and Physics*, 64th ed.; CRC Press: Boca Raton, FL, 1983.

(52) (a) Streitwieser, A., Jr.; Williams, J. E.; Alexandratos, S.; McKelvey, J. M. *J. Am. Chem. Soc.* **1976**, *98*, 4778. (b) Schleyer, P. v. R. *Pure Appl. Chem.* **1984**, *56*, 151. (c) Bader, R. F. W.; MacDougall, P. J. *J. Am. Chem. Soc.* **1985**, *107*, 6788.

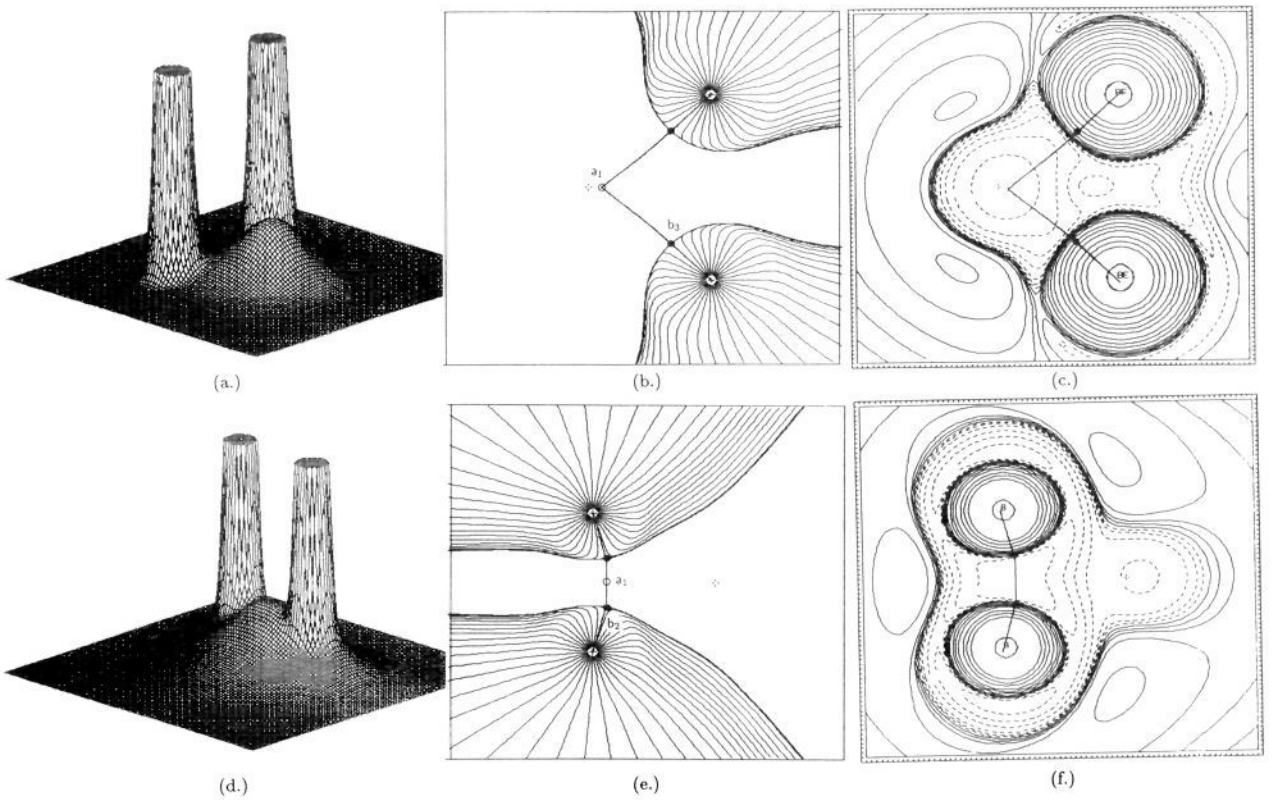

Figure 2. Display of (a) the relief map of the electronic charge densities ρ, (b) its associated gradient vector field of the charge density in terms of paths traced out by the vectors $\nabla\rho$, and (c) the contour map of the Laplacian concentration of the charge density $\nabla^2\rho$ in the plane of the two berylliums and bisecting the B–B bond of **1s** at the MP2/6-31G* level of approximation. Dashed lines in (c) denote negative values of $\nabla^2\rho$ and indicate regions where electronic charge is concentrated. The gradient vector field and the Laplacian concentrations are overlaid with the molecular graphs in the projected plane. Bond paths are indicated by heavy lines and bond critical points by dots. The ring critical points and nonnuclear attractors are indicated by triangles and circles, respectively. The corresponding displays of ρ, $\nabla\rho$, and $\nabla^2\rho$ for the plane containing the two borons and bisecting the berylliums are shown in (d)–(f), respectively.

soft curvatures λ_2, which indicate diffusion of charge density in the plane containing both borons. Additional information is obtained from the Laplacian of the electron density. The large positive value of 8.65 e Å^{-5} for $\nabla^2\rho$ at the bond critical points $\mathbf{r}_{b3}$ suggests that both beryllium atoms donate considerable charge density to the B–B bond (Figure 2c). The question then arises as to whether the Be atoms are complexed ionicly. The negative values of the total energy density $H(\mathbf{r})$ at the two bond critical points $\mathbf{r}_{b3}$, however, imply concentration of charge and covalent bonding. Hence, it is evident that the two beryllium atoms are covalently bonded to the B–B bond by means of two "orthogonal" highly polar π complexes.

Having addressed the bonding of the berylliums, we now focus on that of the borons. Figure 2e displays the charge density gradient field for the plane containing the two boron atoms and bisecting the beryllium bond paths. The two borons are linked to the nonnuclear attractor $\mathbf{r}_{a1}$ via bond paths that each contain bond critical points $\mathbf{r}_{b2}$. The charge density (1.231 e Å^{-3}) of the psuedoatom $\mathbf{r}_{a1}$ is only marginally higher than that of the bond critical points $\mathbf{r}_{b2}$ (1.200 e Å^{-3}) at MP2/6-31G*. The relief map of $\nabla^2\rho$ (Figure 2f) shows that there is an expanded "cylindrical" region where the electron density is rather flat between the two covalently bonded borons; i.e., both H and $\nabla^2\rho$ have negative values at $\mathbf{r}_{a1}$ and $\mathbf{r}_{b2}$. The bond order of 1.22 supports the multiple-bond character of the B–B bond.[53]

The presence of nonnuclear attractors in **1s** and the other structures needs to be addressed because they are currently not well understood. They have been found in the ground states of the diatomics Be_2, Li_2, C_2, and their cations,[41b] in Li_n clusters,[1,4] and in Na_n clusters.[4] Also multiple-bonded hydrocarbons and silicon derivatives can have (3, −3) critical points, but these disappear at higher levels of theory.[54] Therefore, the electron density analysis on **1s** was performed at more complete basis sets to determine whether the presence of $\mathbf{r}_{a1}$ is spurious and basis set dependent. However, at all levels, i.e., HF/6-31G(2d), HF/6-31+G(2d), MP2/6-31G*, MP2/6-31+G(2d), MP2/6-311G*, and MP2/6-311G(df), the nonnuclear attractor remains but shows differences in charge density between $\mathbf{r}_{a1}$ and $\mathbf{r}_{b2}$ that vary from 0.014 to 0.001, to 0.031, to 0.001, to 0.013, and to 0.019 e Å^{-3}, respectively. Thus, these calculations at higher levels of theory do not simplify the topology of **1s** (nor of **2s** and **3s**, see later). Although it cannot be excluded that the nonnuclear attractors disappear with more complete basis sets that include, e.g., more diffuse function and (triply) split basis for all electrons, which were beyond our capabilities, their (non)existence has, however, no effect on the structural and energetic properties of B_2Be_2 species, which is the topic of this paper.

Geometrical distortion, and in particular those of the berylliums, render further insight in the intrinsic stability of the tetrahedron. The rhombic structure **2s** represents the maximum distortion to planarity from the Be–X–Be angle of 80.1° in **1s**. Figure 1 shows the MO diagrams of Be complexation in orthogonal planes (**1s**) versus bonding in one plane (**2s**). The energy difference between **1s** and **2s** of 12.1 kcal/mol (MP4/6-31G*//MP2/6-31G*) is significant and results largely from the stabilizing Be–Be interactions in **1s** (MOs $5(a_1)$, $6(b_1)$, and $8(a_1)$). This is also reflected in the Be–X–Be angle of 80.1° and the charge accumulation in the Be–Be region (Figure 2c), even though this is evidently not enough to result in formal bonding as discussed above. Structure **2s** shows a high sensitivity to the theoretical level employed.

At the correlated MP2/6-31G* level **2s** represents the transition for "inversion" of the tetrahedron as suggested by the normal mode

(53) A bond order of 1.33 is obtained at the HF/6-31G* level of theory.

(54) Boatz, J. A.; Gordon, M. S. *J. Phys. Chem.* **1988**, *92*, 3037.

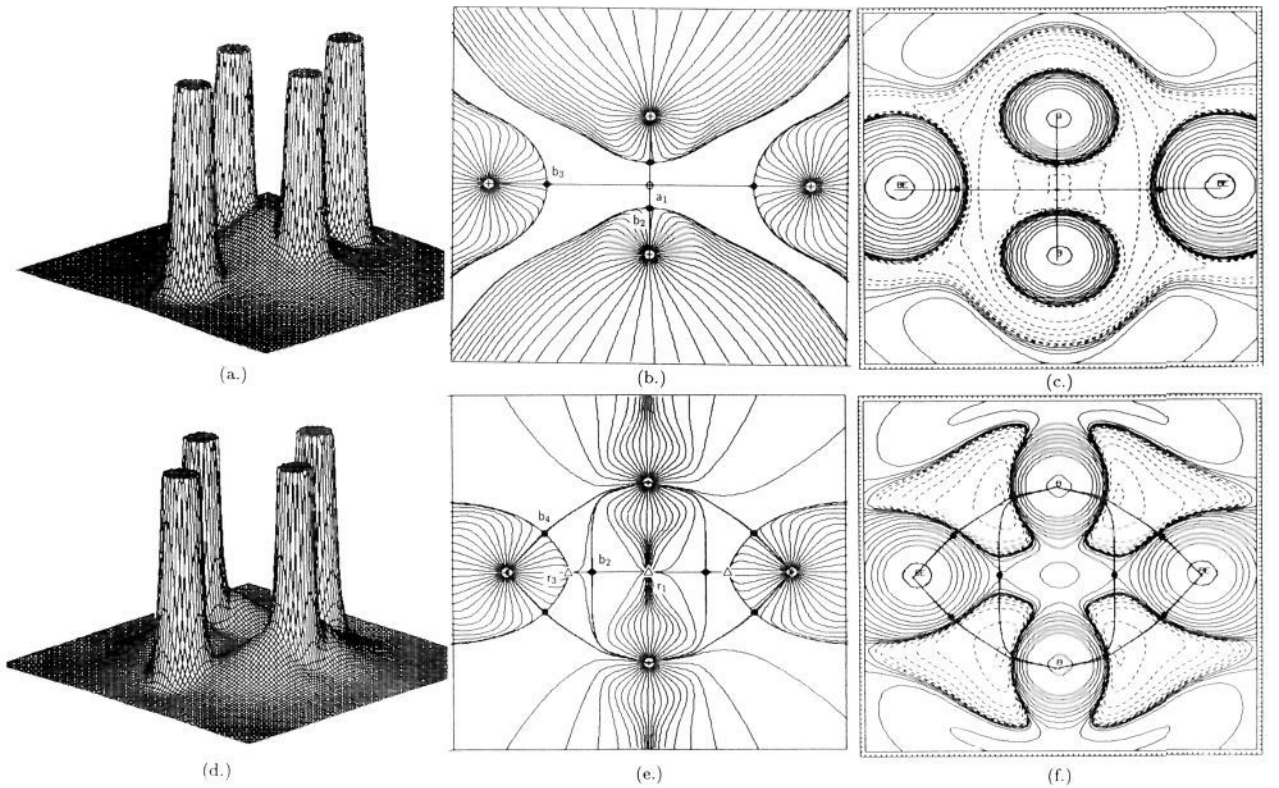

Figure 3. Display of (a) the relief map of ρ, (b) the gradient vector field $\nabla\rho$, and (c) the contour map of the Laplacian $\nabla^2\rho$ of **2s** at MP2/6-31G*. The corresponding displays of ρ, $\nabla\rho$, and $\nabla^2\rho$ for **3s** at MP2/6-31G* are shown in (d)–(f), respectively.

of its (small) imaginary frequency of 60 cm^{-1}. At the HF level **2s** has two imaginary frequencies (Table III), and the transition structure is found to have a C_{2h} geometry (**2s'**, parallelogram). The energy difference between **2s** and **2s'** is marginal and actually reflects a planar flexibility of the complexed berylliums. The electronic detail of **2s** and **2s'** is similar to that of **1s** as revealed by the charge density gradient field and the Laplacian of **2s** (Figure 3; Table IV), which show that both berylliums have bond paths to the center of the B–B bond where the nonnuclear attractor ($\mathbf{r}_{a1}$) is located. The positive $\nabla^2\rho$ and negative H values of the bond critical points $\mathbf{r}_{b3}$ and the soft curvatures λ_2 ($\mathbf{r}_a$, $\mathbf{r}_{b1,2}$) show that the berylliums in **2s** also are π-complexed (polar covalent) to the B–B bond. Also, the electron density analysis of the D_{2h} symmetry structure **2s** underlines its extreme sensitivity to the theoretical level employed. While the HF (NIMAG = 2) and MP2/6-31G* (NIMAG = 1) geometries are nearly identical, their molecular graphs are entirely different. In contrast to the MP2 described π complexation, the HF electron density analysis shows peripheral Be–B bonding and a "split" B–B bond, somewhat similar to the bond-stretch isomer **3s** described below.[55] Evidently, **2s** is a topologically unstable structure at the HF level and cautions to use the appropriate theoretical levels when discussing electronic effects in detail.

Bond-Stretch Isomerism. A second rhombic structure **3s**, which was characterized as a HF/6-31G* local minimum, shows an impressive 50.9 kcal/mol (MP2/6-31G*) energy difference with **2s**. At first glance the major difference between these two structures is the B–B bonding, which differs by 0.335 Å. The relationship between **2s** and **3s** is reminiscent of bond-stretch isomerism,[56] albeit that **2s** is not a minimum. From analysis of the HF/6-31G* MO diagrams (Figure 1), it becomes evident that stretching the B–B separation in **2s** eliminates the B–B bond, while this simultaneously forms the Be–B bonds at the circumference of the rhombic structure. The resulting isomer **3s** is exactly the one predicted by eliminating two electrons (or replacing C for B) from the reported rhombic C_2Be_2 structure,[11,13] which does have Be–C bonds in addition to a C–C bond.

The electron density analysis of **3s** supports the above interpretation but also adds interesting observations that warrant further discussion. The data in Table IV and their graphical representation in Figure 3 demonstrate the significant difference in electronic properties between structures **2s** and **3s**. While **2s** has its electron density mainly concentrated toward the center of the molecule, the electronic charge in **3s** is located at the circumference of the structure. The data show clearly that these B–Be bonds are of polar covalent character and that there is lack of direct B–B bonding. Despite this, Figure 3d–f and Table IV also show that the two borons in **3s** are still connected to each other by two bond paths that are both very strongly curved toward the berylliums. The distances between the bond critical points $\mathbf{r}_{b2}$ on the two B–B bond paths and the central ring critical point $\mathbf{r}_{r1}$ amount to a large 0.592 Å! However, the bond orders for these B–B bond paths are negligible; i.e., $n = 0.03$. This and the similar electron densities ($\Delta\rho$ = 0.052 e $Å^{-3}$) of the bond ($\mathbf{r}_{b2}$) and ring ($\mathbf{r}_{r1}$) critical points effectively indicate a rather flat plateau within the rhombic frame. Nevertheless, the existence of the twin MED bond paths between the borons together with their negative $H(\mathbf{r})$ values satisfies Bader and Cremer's "necessary" and "sufficient" conditions for the existence of a bond.[40,44,46]

(55) It is informative to summarize the main features of the critical points determined for rhombic **2s** and parallelogram **2s'** at HF/6-31G*. Structure **2s'** has similar characteristics to **2s** at MP2/6-31G* (both NIMAG = 1), with only bond paths connecting to a central nonnuclear attractor. Structure **2s** at HF/6-31G* (NIMAG = 2) has peripheral bond paths as well as split B–B bond paths, which are connected to each other via a central bond critical point and their zero-flux surfaces coalesce with those of the peripheral bond critical points to give two ring critical points. Moreover, this central bond critical point is connected to the *cage* critical points along their zero-flux path (one in the direction of each boron). An additional four-ring critical point (two above and two below the cage critical points located in the molecular plane) satisfy the topology criteria, i.e., the Poincaré–Hopf relationship $n - b + r - c = 1$.

(56) (a) Jean, Y.; Lledas, A.; Burdett, J. K.; Hoffmann, R. *J. Am. Chem. Soc.* **1988**, *110*, 4506. (b) Schleyer, P. v. R.; Sax, A. F.; Kalcher, J.; Janoschek, R. *Angew. Chem., Int. Ed. Engl.* **1987**, *26*, 364. (c) Kaufmann, E.; Schleyer, P. v. R. *Inorg. Chem.* **1988**, *27*, 3987. (d) Boatz, J. A.; Gordon, M. S. *J. Phys. Chem.* **1989**, *93*, 2888.

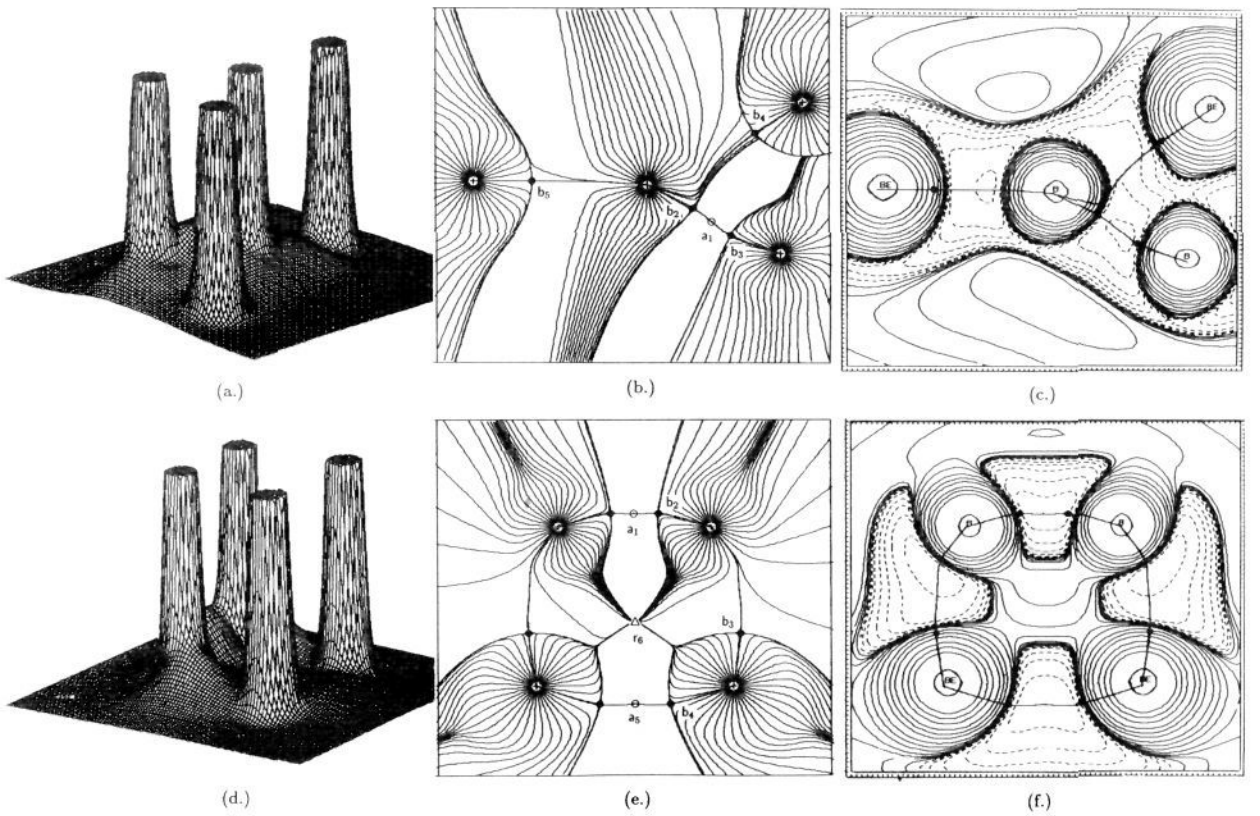

Figure 4. Display of (a) the relief map of ρ, (b) the gradient vector field $\nabla\rho$, and (c) the contour map of the Laplacian $\nabla^2\rho$ of **4s** at HF/6-31G*. The corresponding displays of ρ, $\nabla\rho$, and $\nabla^2\rho$ for **5s** at HF/6-31G* are shown in (d)–(f), respectively.

Apparently this observation of "pseudobonds" is reminiscent of that of pseudoatoms or nonnuclear attractors. Because such critical points may be spurious and dependent on the level of theory employed, single-point calculations were performed on the MP2/6-31G* optimized geometry. The differences in electron density ($\Delta\rho$ in e Å^{-3}, see Figure 3) between the bond critical point $\mathbf{r}_{b2}$ and the ring critical point $\mathbf{r}_{r1}$ (at the center) and $\mathbf{r}_{r3}$ (toward the berylliums and given in parentheses) are 0.052 (0.045), 0.051 (0.028), 0.050 (0.032), and 0.057 (0.041) e Å^{-3} at MP2/6-31G*, MP2/6-31+G(2d), MP2/6-311G*, and MP2/6-311G(df), respectively. There appears to be no indication for the disappearance of $\mathbf{r}_{b2}$. Whether or not pseudobonds (like pseudoatoms) will remain at higher levels of theory is an interesting challenge for further study but is not the topic of this paper.

Other Structures. A variety of other singlet and triplet B_2Be_2 isomers were studied; their structures are displayed, and their energies are tabulated. All species have in common a short B–B distance. However, because none is energetically competitive with the global minimum, we will not elaborate them but only focus on the bonding features of **4s** and **5s** because they are different from those discussed so far.

For example, at HF/6-31G* the trapezoid **5s** (parts d–f of Figure 4) has bonds at all ridges including one between the beryllium atoms of 1.996 Å. In fact, there are two bond critical points $\mathbf{r}_{b4}$ and a nonnuclear attractor $\mathbf{r}_{a5}$ on the Be–Be bond path(!), just like there are on the B–B bond path (i.e., $\mathbf{r}_{b2}$ and $\mathbf{r}_{a1}$). The berylliums are σ-bonded to the borons. However, the relief map of $\rho(\mathbf{r})$ (Figure 4d) illustrates that both the Be–Be and Be–B interactions are very weak as compared to the B–B bond.

Structure **4s** has again a quite different bonding pattern. Only at HF/6-31G* is this Be-substituted B_2Be ring system a transition structure for the interconversion between **5s** and **2s** (or **3s**). The HF/6-31G* electron density analysis (Table IV; parts a–c of Figure 4) shows that also in **4s** the short B–B bond path contains two bond critical points ($\mathbf{r}_{b2}$, $\mathbf{r}_{b3}$) and a nonnuclear attractor ($\mathbf{r}_{a1}$). The 3-membered ring is best viewed as a Be π-complexed (large ϵ) to the B–B bonds, even though the bridging Be has a bond path to the "central" boron and not $\mathbf{r}_{a1}$. This Be–B bond path is *highly concave* and typical for 3c–2e bonds as in hypercoordinated carbocations.[41b,57] The terminal Be is (polar) covalently bonded to the B_2Be unit.

Whereas the linear (triplet) structure is favored by far in the case of C_2Be_2, the contrary is true for (singlet) **8s**, which actually has two imaginary HF/6-31G* frequencies. Several electronic states for the triplet **8t** isomer were investigated, but none proved to be energetically favorable.[58] The $^3\Delta_g$ state is the global minimum at HF, but after inclusion of the effects of electron correlation it is a high-energy isomer.

Energies. The relative B_2Be_2 energies show a mild basis set dependency and a strong influence of the effects of electron correlation as illustrated in Figure 5. Expectantly, all triplet species benefit less from inclusion of electron correlation than singlets do.[32] Thus, while at HF/6-31G*(3-21G) the triplet tetrahedron **1t** is energetically favored over the singlet **1s** isomer by 2.5 (4.9) kcal/mol, the singlet tetrahedron is a significantly 34.7 kcal/mol more stable than the triplet isomer at the correlated level (MP4/6-31G* + ZPE). In fact, at this level all triplet structures are over 30 kcal/mol less stable than the global minimum **1s**. From Figure 5 it also becomes evident that the B–B bridged structures **1s**, **2s**, **4s**, and **6s** benefit most from inclusion of the effects of electron correlation. In fact, this behavior is similar to that well-known for the boranes. For example, the bis(μ-hydrido) B_2H_4 structure (C_{2v}) is energetically competative with its D_{2d} isomer only at the correlated level.[24] It is not surprising, then, that structure **1s** with its two bridging Be atoms benefits most at this level of theory, resulting in an energy difference of over 30 kcal/mol over any other equilibrium B_2Be_2 structure. The increase in energy difference of 36.9 kcal/mol from

(57) For the application of the electron density analysis on carbocations, see: (a) Koch, W.; Frenking, G.; Gauss, J.; Cremer, D. *J. Am. Chem. Soc.* **1986**, *108*, 5808. (b) Bader, R. F. W. *Can. J. Chem.* **1986**, *64*, 1036.

(58) Attempts to obtain a $^3\Sigma_g^-$ isomer resulted in an excited-state species 65 kcal/mol (HF/6-31G*, NIMAG = 0) higher in energy than **1s**.

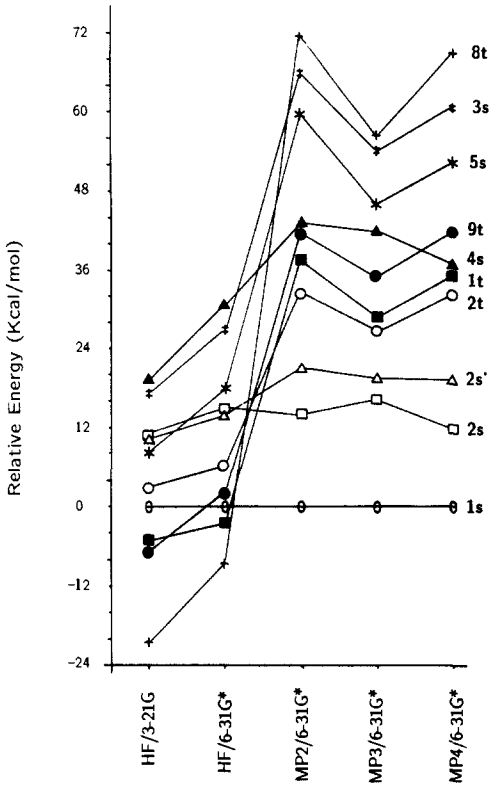

Figure 5. Plot of the relative energies (kcal/mol) vs basis set. All energies are relative to **1s**.

Table VI. Total (au) and Relative (kcal/mol) Energies of MP2/6-31G* Optimized B_2Be_2 Isomers

	1s		2s		3s	
theor level	total	rel	total	rel	total	rel
MCSCF	-78.468 55	0.0	-78.443 27	15.5		
MP2/6-31G*	-78.678 97	0.0	-78.655 67	14.6	-78.574 45	65.6
MP4/6-31G*	-78.695 91	0.0	-78.676 69	12.1		
MP2/6-31+G(2d)	-78.709 66	0.0	-78.685 95	14.9	-78.603 93	66.4
MP2/6-311G*	-78.757 43	0.0	-78.734 13	14.6	-78.653 34	65.3
MP2/6-311G(df)	-78.809 97	0.0	-78.785 97	15.1	-78.705 80	65.4

HF/6-31G* to MP4/6-31G* between the bond-stretch isomer **2s** and **3s** is another display of this effect and in fact supports the structural interpretation presented above. Consequently, the degenerate inversion barrier for the tetrahedron (**1s** $\rightleftharpoons$ **2s** $\rightleftharpoons$ **1s**), which is as expected the least sensitive to the effects of electron correlation, decreases by only 0.8 kcal/mol (HF - MP2/6-31G*). In order to determine more completely the kinetic stability of the tetrahedron **1s**, also single-point MCSCF, MP2/6-31+G(2d) with diffuse sp and two sets of d-type polarization functions, and MP2/6-311G(df) with a set of 6 d-type and 10 f-type functions were carried out for **1s**, **2s**, and **3s** (Table VI). All levels of theory give a similar inversion barrier, which is 14.6 kcal/mol at MP2/6-311G(df) + scaled ZPE.

Table VII. Binding Energies (kcal/mol) for **1s**

reaction	HF/ 3-21G	HF/ 6-31G*	MP2/ 6-31G*	MP4/ 6-31G*
$B_2Be_2 \rightarrow B_2Be + Be$	49.4	60.9	88.2	76.1
$B_2Be_2 \rightarrow B_2 + Be_2$	100.2	111.7	195.4	173.6
$B_2Be_2 \rightarrow B_2 + Be + Be$	100.3	111.9	195.8	173.9
$B_2Be_2 \rightarrow B + B + Be_2$	102.7	122.5	222.6	203.8
$B_2Be_2 \rightarrow B + B + Be + Be$	102.7	122.7	223.1	204.2

Total binding energies (Table VII) reflect the energy difference between a molecule and the atom of which it is composed and are a measure for its intrinsic stability. Assuming that MP4/6-31G* only recovers ca. 90% of the binding energies (as suggested by Raghavachari for C and Si (80–85%)),[59] a scaled value of 226.9 kcal/mol or 9.8 eV is obtained for structure **1s**. The binding energy of one π-complexed Be in **1s** amounts to a scaled value of 84.6 kcal/mol or 3.7 eV.

Conclusions

The important points from the present study can be summarized as follows:

1. The global B_2Be_2 minimum is a tetrahedrallike structure **1s** that is at least 30 kcal/mol more stable than any other isomer.
2. The potential energy surface of this electron-deficient tetraatomic B_2Be_2 cluster shows a large dependency on the inclusion of electron correlation effects.
3. Tetrahedral structure **1s** is best viewed as having its two berylliums π-complexed (in orthogonal planes) to the B–B multiple bond without a Be–Be bond.
4. The inversion barrier of tetrahedral **1s** through a planar D_{2h} form is 14.6 kcal/mol at MP2/6-311G(df)//MP2/6-31G* + scaled ZPE.
5. Bond-stretch isomerism is observed between the two rhombic (D_{2h}) structures **2s** and **3s**. The "crossed" bonds in **2s** change to peripheral bonds in the 50 kcal/mol less stable isomer **3s**.
6. Bader's topological electron density analysis, which is based on the theory of atoms in molecules, shows a high versatility in bonding patterns for B_2Be_2 isomers and includes the observation of nonnuclear attractors and pseudobonds.

Acknowledgment. This work was supported by the United States Air Force Astronautics Laboratory under Contract No. F04611-86-K-0073. We thank Professor R. F. W. Bader for stimulating discussions and for providing us with his programs. P. V. Sudhakar is thanked for his programming assistance. This study benefited from the generous provision of computing time on the Cray X-MP/24 by the Alabama Supercomputer Center.

(59) Raghavachari, K. *J. Chem. Phys.* **1986**, *84*, 5672. Raghavachari, K.; Whiteside, R. A.; Pople, J. A. *J. Chem. Phys.* **1986**, *85*, 6623.